Analysis of Nuclear Scattering by Regge Poles

R. SHANTA AND C. S. SHASTRY*
Saha Institute of Nuclear Physics, Calcutta, India
(Received 23 July 1968)

The validity and usefulness of the complex angular-momentum formulation in nuclear scattering are investigated by studying the elastic scattering of α particles by He^4, C^{12}, and O^{16} in terms of the Regge trajectories through suitable Regge-type representations for the S matrix. The trajectories are obtained from the resonant levels of the compound nuclei, and residues are calculated by imposing unitarity on the Regge-type representations for the S matrix. The differential cross sections obtained by this method are compared with those obtained by experiment and by the Ackhiezer-Pomeranchuk-Blair-McIntyre model with resonant phase shifts. In order to establish the merit of the Regge-pole approach, cross sections are calculated in terms of the poles of the S matrix in the momentum plane and compared with the results obtained by using the complex angular-momentum formulation. These studies provide an interesting method for the analysis of nuclear scattering.

I. INTRODUCTION

THIS paper contains an analysis of elastic scattering of α particles by spinless charged target nuclei based on the complex angular-momentum formulation of nuclear scattering. Apart from describing a simple and elegant way to analyze the nuclear scattering data that we considered, the motivation for the present work is to establish a formalism for nuclear scattering based on the analyticity and unitarity of the S matrix, one simple enough to be suitable for practical applications. In this connection, one notices the important fact that in spite of the great success of analytic S matrix theory in high-energy physics, it has not met with comparable appeal in nuclear scattering and reactions. The most important formulation of the analytic S matrix theory for nuclear reactions is that of Humblet and Rosenfeld.[1] Even though the theory is mathematically elegant and gives the description of the reaction phenomena in terms of the singularities of the S matrix, it has a number of limitations as far as practical applicability is concerned. For example, Rosenfeld's theory assumes that the S matrix is a meromorphic function of momentum and therefore represents it in terms of a Mittag-Leffler expansion containing pole terms and an analytic background part. But it is well known that the S matrix is meromorphic only for a restricted class of potentials and this excludes even the Yukawa potential. For, in the case of Yukawa-type potentials, the S matrix has cuts in addition to pole terms. Therefore, a nuclear-reaction theory based only on poles in the momentum plane is, to some extent, unrealistic. Secondly, the S matrix has, in general, an infinite number of poles for a given angular momentum. As a result, one has to study the S matrix for each partial wave in terms of a large number of poles and an analytic function which is difficult to determine. Finally, the pole terms in the representation for the S matrix in the momentum plane do not have well-known physical properties such as threshold behavior in momentum and asymptotic behavior in angular momentum. Therefore, it is not surprising that such a representation for the S matrix does not generate correct physical partial-wave amplitudes. The elegance of the complex angular-momentum approach[2] lies in removing most of the above-mentioned difficulties, thus providing a practically useful method to analyze nuclear-scattering problems.

In the complex angular-momentum plane ($l=\lambda-\frac{1}{2}$), the analytic properties of the S matrix are simpler than those in the momentum plane. For example, in the case of Yukawa potential, the S matrix is a meromorphic function in the λ plane, physically meaningful poles corresponding to bound states and resonances are always restricted to the right half-plane, and the number of poles is finite for a given positive energy. Secondly, in the complex angular-momentum approach, the full scattering amplitude is usually represented in terms of a few poles in the right half-plane and a background integral. This should be compared with the fact that in the momentum-plane approach, the S matrix for each partial wave is represented in terms of poles and a background term. In contrast to the momentum-plane approach, the background integral in Regge-pole theory represents the effect of singularities in the left-half λ plane, and it is possible to modify the Regge-type representations for poles in such a way that the effect of the background integral is reduced. This is perhaps the most striking achievement of the complex angular-momentum approach over the momentum-plane approach. Another very satisfying feature of the complex angular-momentum theory is the following: It is possible to formulate Regge-type representations for partial-wave amplitudes such that in addition to keeping the background effect small, they exhibit the physical features of the S matrix: namely, correct threshold behavior in momentum, asymptotic behavior in angular momentum, and unitarity. Thus what one achieves is a representation of the S matrix (in terms of poles in the complex angular-momentum plane) which has all the necessary physical features and small background effects. These features support the idea that a

* Present address: Louisiana State University, Baton Rouge, La. 70803.

[1] J. Humblet and L. Rosenfeld, Nucl. Phys. **26**, 529 (1961).

[2] T. Regge, Nuovo Cimento **14**, 951 (1959); **18**, 947 (1960).

nuclear-scattering theory based on Regge poles can be expected to be useful for practical applications.

The application of Regge-pole theory to nuclear scattering was first studied by Rebolia and Viano[3] and by a series of subsequent investigators.[4–6] In these works it was shown that by treating Regge poles and residues as parameters, one can fit by the method of least squares α-C^{12} scattering data in terms of a Regge representation. In these calculations the background integral was assumed to be zero. Considering the interesting results of these initial calculations, the formulation of nuclear scattering based on Regge poles was systematically investigated. In particular, its applicability to charged particle scattering,[7,8] which becomes complicated due to the presence of Coulomb force in addition to nuclear interaction, was established. It was found[8] that the analytic properties of the Coulomb-nuclear S matrix are such that one can study the "nuclear amplitude," which is the difference between the full amplitude and the Coulomb amplitude, by usual Regge-pole techniques. Various Regge-type representations were tested for the S matrix both for pure nuclear[9–11] scattering and Coulomb-nuclear[12] scattering. It was shown that in the low-energy region, corresponding to nuclear scattering, it is possible to formulate very good representations generating the partial-wave amplitudes almost quantitatively. It should be noted that the pole parameters obtained in the earlier calculations[3–6] referred to above may not be reliable, because the background integral which was neglected as an approximation need not be small. The present paper deals with the problem along the lines discussed earlier. In order to do this the levels of the compound nuclei are categorized in terms of Regge trajectories, and in doing this we use the well-known salient features of Regge trajectories. The residues of the poles are then obtained by imposing unitarity for the Regge-type representation for the partial-wave amplitude and, based on these pole parameters and suitable representations, differential cross sections are calculated. The resonant states of the compound nuclei and the resonance widths are not taken as parameters. The only factors used other than the energy levels and widths of the compound nucleus are the radius of the compound nucleus and a diffuseness parameter, which were given some suitable fixed values and were not treated as parameters in the calculations.

In Sec. II we give a brief discussion of Regge-type representations for the partial-wave amplitudes formulated, and the method of calculation is discussed. In Sec. III the levels of the compound nuclei such as Be^8, O^{16}, and Ne^{20} are categorized in terms of Regge trajectories for α-α, α-C^{12}, and α-O^{16} systems, respectively, and discussed. Section IV contains the results of various calculations and discussions.

II. REGGE-TYPE REPRESENTATIONS FOR CHARGED-PARTICLE PARTIAL-WAVE AMPLITUDE

In the notation of Lane and Thomas,[13] the scattering amplitude $A(k, \cos\theta)$ for the scattering of two spinless charged particles, of charge Z_1e and Z_2e, is given by

$$A(k,\cos\theta)=(2k)^{-1}[-\eta\csc^2\tfrac{1}{2}\theta\exp(-2i\eta\ln\sin\tfrac{1}{2}\theta)+i\sum_{l=0}^{\infty}(2l+1)(e^{2i\omega_l}-U_l)P_l(\cos\theta)] \quad (2.1)$$

$$=(2k)^{-1}[-\eta\csc^2\tfrac{1}{2}\theta\exp(-2i\eta\ln\sin\tfrac{1}{2}\theta)]+A_{\rm nuc}(k,\cos\theta). \quad (2.2)$$

In this expression, U_l is given by

$$U_l=e^{-2i\sigma_0}S_l(k)=e^{2i(\sigma_l-\sigma_0)}\bar{S}_l(k), \quad (2.3)$$

where σ_l is the Coulomb phase shift for the lth partial wave. In terms of the charge parameter $\eta=Z_1Z_2e^2/\hbar v$, the Coulomb phase shift is

$$\omega_l=\sigma_l-\sigma_0=\sum_{m=1}^{l}\tan^{-1}\frac{\eta}{m}. \quad (2.4)$$

The quantities $\bar{S}_l(k)$ and $S_l(k)$ of Eq. (2.3) are the nuclear and full S matrix, respectively. For the Yukawa-type nuclear potentials it can be shown that for $k>0$, the asymptotic behavior of $\bar{S}(\lambda,k)$, i.e., the analytically continued $\bar{S}_l(k)$ in the λ $(=l+\frac{1}{2})$ plane, is given by[8]

$$|\bar{S}(\lambda,k)-1|=O(|\lambda^{-1/2}e^{-{\rm Re}\lambda\xi}|), \quad |\lambda|\to\infty,\ {\rm Re}\lambda\geqslant 0, \quad (2.5)$$

where

$$\xi=\cosh^{-1}(1+\mu_0^2/2k^2), \quad (2.6)$$

and μ_0^{-1} is the highest value of the range appearing in a superposition of Yukawa potentials. Using this asymptotic property, one may perform a Sommerfeld-Watson (SW) transform on the function

$$\bar{A}(k,\cos\theta)=(2ik)^{-1}\times\sum_l(2l+1)[\bar{S}(\lambda,k)-1]P_l(\cos\theta), \quad (2.7)$$

[3] L. Rebolia and G. A. Viano, Nuovo Cimento **26**, 1426 (1962).
[4] M. Carrassi and G. Passatore, Nuovo Cimento **32**, 1337 (1964).
[5] M. Bertero, M. Carrassi, and G. Passatore, Nuovo Cimento **36**, 954 (1965).
[6] V. V. Grushin and Yu. P. Nikitin, Yadern. Fiz. **5**, 173 (1967) [English transl.: Soviet J. Nucl. Phys. **5**, 122 (1967)].
[7] S. Klarsfeld, Nuovo Cimento, **48**, 1059 (1967).
[8] S. Mukherjee and C. S. Shastry, Nucl. Phys. **B3**, 1 (1967).
[9] W. J. Abbe, P. Kaus, P. Nath, and Y. N. Srivastava, Phys. Rev. **140**, 1595 (1965).
[10] W. J. Abbe and G. A. Gary, Phys. Rev. **160**, 1510 (1967).
[11] S. Mukherjee and C. S. Shastry, Phys. Rev. **169**, 1234 (1968).
[12] C. S. Shastry and R. K. Satpathy, Phys. Rev. **175**, 1544 (1968).
[13] A. M. Lane and R. G. Thomas, Rev. Mod. Phys. **30**, 257 (1958).

and obtain the following Regge representation:[2]

$$\bar{A}(k,\cos\theta)=(2i)^{-1}\int_{-i\infty}^{+i\infty}d\lambda'\frac{2\lambda' P_{\lambda'-1/2}(-\cos\theta)}{\cos\pi\lambda'}a(\lambda',k)+\sum_{n=1}^{N}\frac{2\pi\lambda_n\beta_n P_{\lambda n-1/2}(-\cos\theta)}{\cos\pi\lambda_n}, \quad (2.8)$$

where $a(\lambda,k)=[\bar{S}(\lambda,k)-1]/2ik$. Here λ_n denotes the pole position, N is the total number of poles in the right-half λ plane, and β_n is the residue of $a(\lambda,k)$ at $\lambda=\lambda_n$. Neglecting the background integral in Eq. (2.8), after partial-wave projection one obtains

$$a(\lambda,k)=\sum_{n=1}^{N}\frac{2\lambda_n\beta_n}{\lambda^2-\lambda_n{}^2}. \quad (2.9)$$

Alternatively, one could perform the SW transform for $A_{\text{nuc}}(k,\cos\theta)$ of Eq. (2.2) and obtain, in the pole approximation, the representation

$$S_c(\lambda,k)a(\lambda,k)=\sum_n \beta_n S_c(\lambda_n,k)\frac{2\lambda_n}{(\lambda^2-\lambda_n{}^2)}, \quad (2.10)$$

where $S_c(\lambda,k)$ is the Coulomb S matrix, i.e., $e^{2i\sigma_l}$.

However, calculations performed[12] on representations of the type given by Eq. (2.10) show that they are not better than the representations of the type given by Eq. (2.9). Therefore, in this paper we restrict ourselves to the representations for $a(\lambda,k)$ only.

When one attempts to analyze nuclear scattering in terms of Regge poles corresponding to the physical states of the interacting system, it is evident that only the poles in the right-half λ plane are to be considered. It is then desirable to formulate the Regge-type representations for the partial-wave amplitude which are capable of generating the exact phase shifts in terms of the poles and residues in the right-half λ plane. In general, representations of this kind can be expressed in the form[14]

$$a(\lambda,k)=\sum_n \beta_n\frac{F(\lambda_n,\lambda)}{\lambda-\lambda_n}+\int_{-i\infty}^{+i\infty}d\lambda'\frac{F(\lambda',\lambda)}{\lambda-\lambda'}a(\lambda',k), \quad (2.11)$$

where $F(\lambda',\lambda)$ is such that $F(\lambda,\lambda)=1$ and $F(\lambda',\lambda)$ is analytic for $\mathrm{Re}\lambda\geqslant 0$, $\mathrm{Re}\lambda'\geqslant 0$; furthermore, $F(\lambda',\lambda)\times a(\lambda',k)$ is bounded on the right half of the λ' plane, so that the integral in Eq. (2.11) can be evaluated by closing the contour in that half-plane. Generally, $F(\lambda',\lambda)$ is constructed such that the pole terms in Eq. (2.11) have correct threshold behavior in k, asymptotic behavior in λ, and the background integral, which manifests the effect of all the singularities in the left-half λ plane, is damped. In the Coulomb-nuclear problem, in addition to the usual threshold properties of the partial-wave amplitude, it is desirable to incorporate the Coulomb threshold factor[15]

$$\mathcal{E}_{\lambda-1/2}{}^2=e^{-\pi\eta}\frac{\Gamma(\lambda+\frac{1}{2}+i\eta)\Gamma(\lambda+\frac{1}{2}-i\eta)}{[\Gamma(\lambda+\frac{1}{2})]^2}. \quad (2.12)$$

Thus $F(\lambda',\lambda)$ has the following forms for the different representations:

$$F(\lambda',\lambda)=\frac{2\lambda}{\lambda+\lambda'}\frac{\mathcal{E}_{\lambda-1/2}{}^2}{\mathcal{E}_{\lambda'-1/2}{}^2}, \quad (2.13)$$

corresponding to Regge representation, and

$$F(\lambda',\lambda)=e^{(\lambda'-\lambda)\xi}\mathcal{E}_{\lambda-1/2}{}^2/\mathcal{E}_{\lambda'-1/2}{}^2, \quad (2.14)$$

corresponding to Khuri representation.[16] For the modified Regge representation of Ref. 14, we write

$$F(\lambda',\lambda)=\left(\frac{2\lambda}{\lambda+\lambda'}\right)^m\left(\frac{\exp(ie^{-\lambda}\xi)-1}{\exp(ie^{-\lambda'}\xi)-1}\right)\frac{\mathcal{E}_{\lambda-1/2}{}^2}{\mathcal{E}_{\lambda'-1/2}{}^2}, \quad (2.15)$$

where m is a suitable positive integer. The first factor in Eq. (2.15) is expected to make the background integral small for large λ'; the second factor reproduces correct threshold behavior in k and asymptotic behavior in λ. The last factor introduces correct Coulomb threshold behavior.

It is well known that the nuclear-scattering potential has a Saxon-Woods radial dependence with the form

$$V(r)=e^{-r/a_0}(e^{-r/a_0}+e^{-R/a_0}). \quad (2.16)$$

Here R is the radius parameter and a_0 is the diffuseness parameter. The radius R is of the order

$$R=(1.45A^{1/3}+1.3)\ \mathrm{F}, \quad (2.17)$$

which is the form used by Carter *et al.*,[17] and a_0 is of the order of 0.55 F. In our calculations we found that it was desirable to incorporate the effect of the parameters R and a_0 of the nuclear potential in constructing a representation for nuclear scattering. For example, in the case of scattering of two spinless uncharged particles, the asymptotic behavior of $a(\lambda,k)$ along the real axis is determined by the integral[18]

$$I=\int_0^\infty rV(r)J_\lambda{}^2(kr)dr. \quad (2.18)$$

Using Eq. (2.16) for $V(r)$ and since the impact parameter λ/k lies in the interval $[0,\infty]$, we have by mean value theorem

$$I\sim(e^{-\lambda/ka_0}+e^{-R/a_0})^{-1}\int_0^\infty re^{-r/a_0}J_\lambda{}^2(kr)dr \quad (2.19)$$

[14] S. Mukherjee, Phys. Rev. **160**, 1546 (1967).

[15] P. B. Treacy, Nucl. Phys. **A96**, 145 (1967).

[16] N. N. Khuri, Phys. Rev. **130**, 429 (1963).

[17] E. B. Carter, G. E. Mitchell, and R. H. Davis, Phys. Rev. **133**, B1420 (1964).

[18] V. De Alfaro and T. Regge, *Potential Scattering* (North-Holland Publishing Co., Amsterdam, 1965).

$$=(e^{-\lambda/ka_0}+e^{-R/a_0})^{-1}\left(-\frac{1}{\pi k}\right)\frac{d}{d(a_0^{-1})}Q_{\lambda-1/2}\times\left(1+\frac{1}{2a_0^2k^2}\right). \quad (2.20)$$

From the asymptotic behavior of the second Legendre function[18] for large λ, it follows that

$$I=(e^{-\lambda/ka_0}+e^{-R/a_0})^{-1}O[|\lambda|^{1/2}\exp(-\lambda\bar{\xi})], \quad (2.21)$$

where

$$\bar{\xi}=\cosh^{-1}(1+1/2a_0^2k^2).$$

Note that the term $e^{-\lambda/ka_0}+e^{-R/a_0}$ does not change the dominant asymptotic behavior; it gives only a somewhat more explicit form of the asymptotic behavior, and the inclusion of this factor was found to be very useful. Thus the new form is

$$F(\lambda',\lambda)=e^{(\lambda'-\lambda)\bar{\xi}}\frac{\lambda(e^{-\lambda'/ka_0}+e^{-R/a_0})}{\lambda'(e^{-\lambda/ka_0}+e^{-R/a_0})}\frac{\mathcal{E}_{\lambda-1/2}{}^2}{\mathcal{E}_{\lambda'-1/2}{}^2}, \quad (2.22)$$

corresponding to Eq. (2.14), and we shall designate this representation as NK. The new form of $F(\lambda',\lambda)$ corresponding to Eq. (2.15) is

$$F(\lambda',\lambda)=\left(\frac{2\lambda}{\lambda+\lambda'}\right)^m\left(\frac{\exp(ie^{-\lambda}\xi)-1}{\exp(ie^{-\lambda'}\xi)-1}\right)\times\frac{\lambda(e^{-\lambda'/ka_0}+e^{-R/a_0})}{\lambda'(e^{-k/ka_0}+e^{-R/a_0})}\frac{\mathcal{E}_{\lambda-1/2}{}^2}{\mathcal{E}_{\lambda'-1/2}{}^2}, \quad (2.23)$$

and we shall designate this representation as N_m.

Another modification which was shown to be extremely useful was to incorporate the unitarity of $\tilde{S}(\lambda,k)$ at $\lambda=\lambda_n{}^*$. In order to do this we follow the procedure of Ref. 11 and obtain for the partial-wave amplitude

$$a(\lambda,k)=\sum_{n=1}^{N}\beta_n\frac{F(\lambda_n,\lambda)}{\lambda-\lambda_n}\frac{\prod_m(\lambda-\lambda_m{}^*)}{\prod_m(\lambda_n-\lambda_m{}^*)}\left(\frac{2\lambda_n}{\lambda+\lambda_n}\right)^N$$

$$-\frac{1}{2ik}\sum_{n=1}^{N}F(\lambda_n{}^*,\lambda)\frac{\prod_{m\neq n}(\lambda-\lambda_m{}^*)}{\prod_{m\neq n}(\lambda_n{}^*-\lambda_m{}^*)}\left(\frac{2\lambda_n{}^*}{\lambda+\lambda_n{}^*}\right)^N, \quad (2.24)$$

where the number of terms in the above product depends upon the number of zeros of $\tilde{S}(\lambda,k)$. It is clear that all the above representations express the partial-wave amplitudes as sum over the pole terms. There is another class of representations, namely, Cheng-type product representations.[9,19] It was found that for sufficiently weak potentials a modified Cheng representation (MC) gives extremely good results but was found to be not satisfactory for lower partial waves. Another important drawback in the MC is that it presumes the knowledge of the Born term, which means that in order to construct an MC a detailed knowledge of the potential is necessary. Considering these facts, we did not formulate the representation MC corresponding to our problem. In nuclear-scattering problems, potentials are not known uniquely, and it may not be possible to derive Born terms corresponding to these potentials in closed form. As a result, the representation MC is not easily applicable to nuclear-scattering problems. Even if the form of the potential is known, in using the MC we lose the important point stressed in the present approach, namely, the analysis of nuclear scattering only in terms of the Regge poles, without detailed reference to the potential.

From the above discussion it is evident that once we have knowledge of the poles and residues we may obtain the differential cross sections of a given nuclear scattering using appropriate Regge-type representations. In order to obtain the positions of the poles from the positions and widths of the resonances of the system we can use the method adopted by Treacy.[15] More details of this with respect to α-α, α-C^{12}, and α-O^{16} systems are described in Sec. III. In order to obtain the residues for the poles we can use unitarity at $\lambda=\lambda_n{}^*$. If we neglect the background integral in Eq. (2.11) and use the elastic unitarity of the S matrix,

$$S(\lambda,k)S^*(\lambda^*,k^*)=1, \quad (2.25)$$

we obtain the following set of linear equations in β_n:

$$\frac{-1}{2ik}=\sum_{n=1}^{N}\beta_n\frac{F(\lambda_n,\lambda_m{}^*)}{\lambda_m{}^*-\lambda_n}, \quad m=1, 2, \cdots, N. \quad (2.26)$$

If the representation that we use is good enough at low energies, the solution of Eq. (2.26) is found to give fairly accurate values for the residues. In this connection it should be noted that the imposition of unitarity at $\lambda=\lambda_n{}^*$ in Eq. (2.24) cannot give expressions for β_n in terms of poles, because in the construction of this representation, unitarity at $\lambda=\lambda_n{}^*$ is already built in.

Summarizing, in the formulation of the above scheme for nuclear scattering we have made use of the fact that the scattering potential has generally Saxon-Woods radial dependence. Then we conjectured that the resonant states of the scattering can be catagorized in terms of Regge trajectories in the right-half λ plane. Using the unitarity of the S matrix, we then obtained the residues through appropriate Regge-type representations. The set of poles and residues together with a representation depicting all the physical features, and rendering the background integral small, were then used to calculate the differential cross sections.

III. REGGE TRAJECTORIES FOR α-α, α-C^{12}, AND α-O^{16} SYSTEMS

In this section we categorize the excited levels of Be^8, O^{16}, and Ne^{20} in terms of Regge trajectories for the

[19] H. Cheng, Phys. Rev. 144, 1237 (1966).

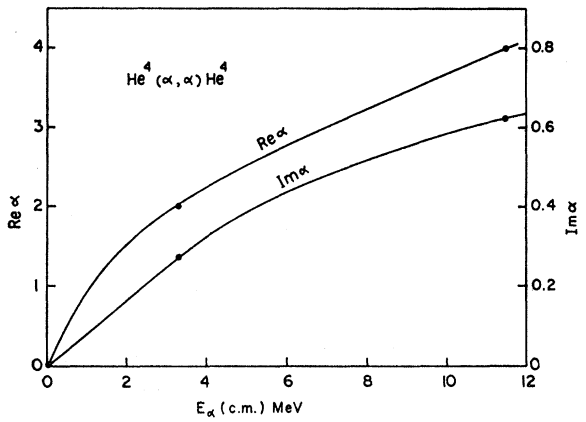

FIG. 1. Regge trajectory for the low-lying levels of Be^8.

α-α, α-C^{12}, and α-O^{16} scattering, respectively. The method that we use is empirical and similar to the procedure of Treacy.[15] In order to do this we take into account the essential features of Regge trajectories. The most important trajectories are those which occur in the right-half λ plane connecting the bound states and resonances. A pole at negative energy and positive half-integer value of λ corresponds to a bound state of angular momentum l. As the energy becomes positive the poles move into the right-half λ plane. In the case of the superposition of Yukawa potentials the trajectories turn back and move towards the left-half λ plane. The poles occurring before this turning point, with a half-integer value for the real part and the small imaginary part, correspond to the resonances. In the case of the superposition of Yukawa potentials, it is found that both the real and imaginary parts of the trajectories in the right-half λ plane increase steadily as they move from the real axis towards the turning point. It can be shown that the width Γ of a resonant state is related to the Regge pole corresponding to it in the following manner[20]:

$$\Gamma = 2\,\mathrm{Im}\lambda_n\left(\frac{d}{dE}\mathrm{Re}\lambda_n\right)\Big/\left(\frac{d}{dE}\mathrm{Re}\lambda_n\right)^2+\left(\frac{d}{dE}\mathrm{Im}\lambda_n\right)^2. \quad (3.1)$$

Considering the above features of Regge trajectories, we determine the Regge trajectories of a nuclear scattering system of two spinless particles as follows: The energy levels forming a trajectory are grouped according to increasing energy and angular momentum. Knowing the resonance energies and corresponding angular momentum values, the real part of the trajectory is drawn, using a graphical method and assuming a polynomial expansion for the real part of the trajectory:

$$\mathrm{Re}\lambda_n = a_0^{(n)}+a_1^{(n)}E+a_2^{(n)}E^2+a_3^{(n)}E^3. \quad (3.2)$$

TABLE I. Level parameters of Be^8 for the Regge trajectory of the α-α system.

E_α(lab) (MeV)	E_x (MeV)	E_α(c.m.) (MeV)	J^π	Γ(c.m.)
0.190	0	0.095	0^+	6.8±1.7 eV
6.55	3.18	3.275	2^+	1.5 MeV
22.99	11.4	11.495	4^+	≃7.0 MeV

TABLE II. Level parameters of O^{16} for the Regge trajectories of the α-C^{12} system.

Trajectory	E_α(lab) (MeV)	E_x (MeV)	E_α(c.m.) (MeV)	J^π	Γ (keV)
I		5.66[a]	−1.49[a]	0^{+a}	
		7.1	−0.05	1^-	
	3.582	9.84	2.69	2^+	1
	11.08	15.45	8.3	3^-	380
	13.9	17.55	10.4	4^+	225
II		6.13	−1.02	3^-	
	4.28	10.36	3.21	4^+	36
	8.15[a]	13.27[a]	6.12[a]	5^{-a}	≃189[a]
	12.1	16.2	9.05	6^+	380
	18.4	20.9	13.75	7^-	750
III	3.24	9.58	2.43	1^-	860
	5.82	11.51	4.365	2^+	106
	11.4	15.1	8.53	3^-	525
	16.13[a]	19.25[a]	12.1[a]	4^{+a}	≃1074[a]
	18.5	21.0	13.85	5^-	1200
IV		6.036	−1.114	0^+	
	7.04	12.43	5.28	1^-	230
	12.35	16.41	9.26	2^+	60
	15.46[a]	18.75[a]	11.6[a]	3^{-a}	≃120[a]
	17.75	20.44	13.29	4^+	150
V		6.92	−0.23	2^+	
	3.066[a]	9.45[a]	2.3[a]	3^{-a}	≃137[a]
	8.97	13.88	6.73	4^+	90
	15.2	18.55	11.4	5^-	190
	18.7	21.2	14.05	6^+	450

[a] Tentative assignments.

TABLE III. Level parameters of Ne^{20} for the first set of Regge trajectories of the α-O^{16} system.

Trajectory	E_α(lab) (MeV)	E_x (MeV)	E_α(c.m.) (MeV)	J^π	Γ (keV)
I	2.46	6.722	1.969	0^+	19
	5.19	8.905	4.152	1^-	23
	7.76[a]	10.963[a]	6.21[a]	2^{+a}	≃49[a]
	9.58	12.39	7.637	3^-	100
	10.87	13.43	8.677	4^+	140
II	1.3	5.79	1.037	1^-	≃2.5
	3.45	7.434	2.681	2^+	10
	7.2	10.49	5.737	3^-	55[a]
	10.546	13.19	8.437	4^+	75
III	0.271	4.97	0.217	2^+	≃2.3
	3.016	7.166	2.413	3^-	10
	5.403	9.076	4.323	4^+	10
	7.88[a]	11.063[a]	6.31[a]	5^{-a}	16.5[a]
	11.483	13.94	9.187	6^+	125
IV	0.037[a]	4.783[a]	0.03[a]	2^{+a}	9[a]
	1.125[a]	5.653[a]	0.09[a]	3^{-a}	269[a]
	2.834	7.02	2.267	4^+	740[a]
	6.934	10.3	5.547	5^-	150
	9.82	12.58	7.827	6^+	130
	11.2	13.69	8.937	7^-	400
	12.137[a]	14.463[a]	9.71[a]	8^{+a}	595.5[a]

[a] Tentative assignments.

[20] R. G. Newton, *Complex j-plane* (W. A. Benjamin, Inc., New York, 1964).

Then, using the known widths of the resonances and the slope of the trajectory,

$$\frac{d}{dE}(\mathrm{Re}\lambda)\,|_{\lambda=\lambda n} \tag{3.3}$$

in Eq. (3.1), $\mathrm{Im}\lambda_n$ is calculated corresponding to each resonance. Then this set of $\mathrm{Im}\lambda_n$ corresponding to various resonances is connected in a smooth way, using a graphical method and assuming a smooth polynomial dependence with respect to energy:

$$\mathrm{Im}\lambda_n = b_0^{(n)} + b_1^{(n)}E + b_2^{(n)}E^2 + b_3^{(n)}E^3. \tag{3.4}$$

This procedure is similar to the one used by Treacy[15] and gives an empirical set of Regge trajectories. From the knowledge of these trajectories and unitarity, the residues for each pole corresponding to various representations can be evaluated, as discussed earlier.

Table I shows the grouping of the three lower levels[21] of Be^8 in order to obtain the Regge trajectory for the α-α system. This is a system of two identical spinless particles obeying Bose-Einstein statistics, and therefore the resonances of elastic scattering occur only at even values of the oribtal angular momentum. Figure 1 shows the Regge trajectory of this system, calculated following the method of Treacy.[15] From the existing data on the levels of Be^8 we obtain only one smooth trajectory.

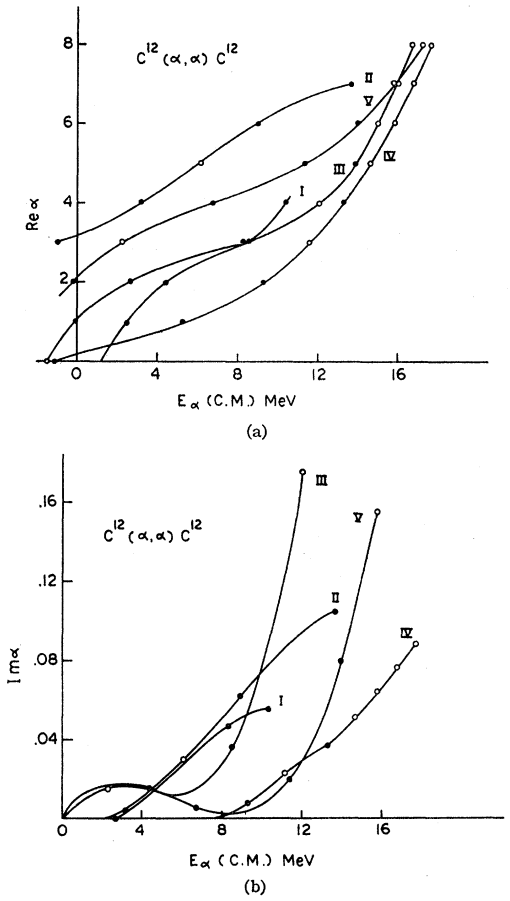

FIG. 2. (a) The real part and (b) the imaginary part of λ_n versus the bombarding energy in c.m. units for the levels of O^{16}. Actually observed levels and tentative levels are indicated by solid and open circles, respectively.

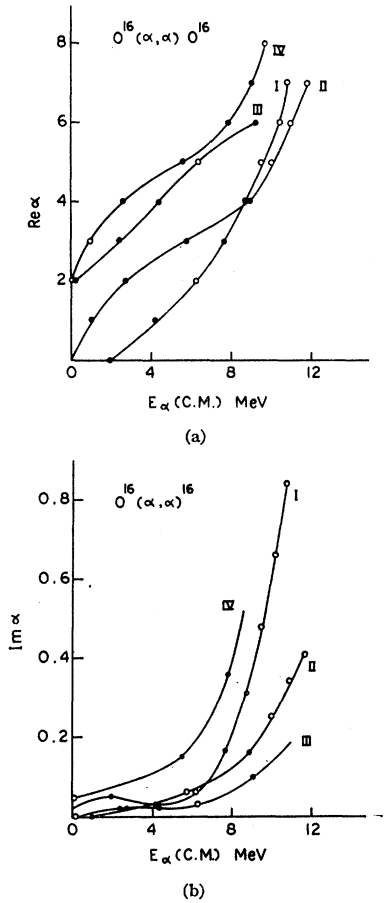

FIG. 3. (a) The real part and (b) the imaginary part of λ_n versus the bombarding energy in c.m. units for the levels of Ne^{20}. The conventions of Fig. 2 are followed.

Table II shows the grouping of energy levels[17,22,23] for O^{16} which mainly decay by α emission, from which we determine the Regge trajectories for the α-C^{12} system. Figure 2 shows these trajectories. The full circles correspond to actually observed levels and the open circles refer to tentative levels. Extrapolation of some of these trajectories in the region where the experimental findings of different resonances and their quantum numbers are inconclusive is interesting. For example, extrapolation of trajectory IV [see Fig. 2(a)] indicates a series of narrow resonances at excitation energies (E_x) 21.8, 22.95, 23.95 MeV, etc. Rasmussen *et*

[21] T. Lauritsen and F. Ajzenberg-Selove, Nucl. Phys. **78**, 1 (1966).

[22] R. W. Hill, Phys. Rev. **90**, 845 (1953).

[23] C. Miller Jones, G. C. Phillips, R. W. Harris, and E. H. Bechnen, Nucl. Phys. **37**, 1 (1962).

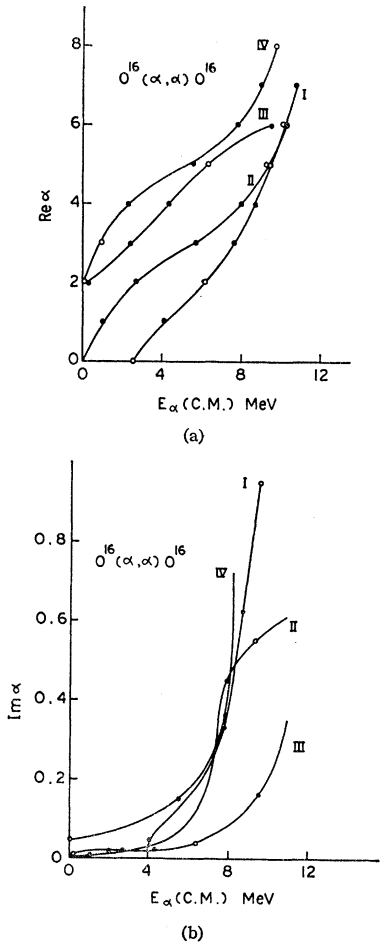

FIG. 4. (a) and (b) the same as for Fig. 3 and corresponding to the grouping of levels in Table IV.

at.[24] observed a resonance at E_α(lab)=21.85 MeV, which indicates the existence of an intermediate state of $C^{12}+\alpha$ at 23.5 MeV. Extrapolation of trajectory V also indicates the presence of excited levels at energies 23 and 24.3 MeV of spin and parity 7^- and 8^+, and approximate widths 635 and 770 keV, respectively. From rotational-band systematics, Carter *et al.*[17] also expected an 8^+ level between 24 and 30 MeV of width approximately equal to 400 keV.

Table III contains the energy levels[25–28] of Ne^{20} grouped in order to obtain the trajectories for the α-O^{16} system. Figure 3 shows these trajectories. When extrapolating trajectory I, it is seen to pass through the levels at excitation energies 14.24, 14.43, and 15.52 MeV of spin and parity 5^-, 6^+, and 7^-, and approximate widths 86, 193, and 212 keV, respectively. Inspection of the results of Mehta *et al.*[28] shows that there are some levels of unassigned spin and parity in this region. For instance, there are energy levels at excitation energies 14.148 and 15.25 MeV of width 150 keV. Trajectory II, on extrapolation, passes through the levels at excitation energies 14.668, 15.693, and 16.483 MeV of spin and parity 5^-, 6^+, and 7^-, respectively. The latter two may correspond to the levels at 15.72 and 16.483 MeV observed by Mehta *et al.*,[28] whose spins and parities were not determined. Trajectory IV passes through a tentative 3^- level at $E_x=5.653$ MeV of width 269 keV. This may well correspond to the 3^- level observed by Pearson *et al.*[27] at 5.62-MeV excitation energy. On extrapolation, trajectory IV passes through an 8^+ level at $E_x=14.463$ MeV. In the work of Mehta *et al.*[28] a level was observed at 14.38 MeV whose spin and parity were not assigned.

At this stage we wish to point out that in general it may not be possible to obtain a unique set of trajectories for a given scattering system, particularly when the compound nucleus has many closely packed energy levels, because, even after restricting ourselves to the general prescription discussed earlier for the choice of the trajectories, one may still be able to obtain more than one set of trajectories. This is, indeed, a limitation of the present procedure. Therefore, in the absence of knowledge of the realistic target-nucleus potential which can generate the actual trajectories, the choice of a particular set of trajectories should be based on the fits that it gives for the experimental data. To illustrate this point we have tabulated in Table IV an alternative grouping of the levels of Ne^{20} which gives a set of trajectories different from the one obtained from Table III. It was found that the trajectories corresponding to Table IV generate the differential cross sections satisfactorily in the incident energy range 7–10 MeV, while

TABLE IV. Level parameters of Ne^{20} for the second set of Regge trajectories of the α-O^{16} system.

Trajectory	E(lab) (MeV)	E (MeV)	E(c.m.) (MeV)	J^π	Γ (keV)
I	5.19	8.905	4.152	1^-	23
	7.7[a]	10.913[a]	6.16[a]	2^+[a]	150
	9.58	12.39	7.637	3^-	100
	10.87	13.43	8.677	4^+	140
	11.837[a]	14.223[a]	9.47[a]	5^-[a]	170[a]
	12.65[a]	14.873[a]	10.12[a]	6^+[a]	≃287[a]
	13.37	15.43	10.677	7^-	470
II	1.3	5.79	1.037	1^-	≃2.5
	3.45	7.434	2.681	2^+	10
	7.2	10.49	5.737	3^-	≃65[a]
	10.05	12.77	8.017	4^+	130
III	0.271	4.97	0.217	2^+	2.5[a]
	3.016	7.166	2.413	3^-	10
	5.403	9.076	4.323	4^+	10
	7.94[a]	11.103[a]	6.35[a]	5^-[a]	≃20.6[a]
	11.97	14.3	9.547	6^+	300
IV	The same as given in Table III				

[a] Tentative assignments.

[24] V. K. Rasmussen, D. W. Miller, and M. B. Sampson, Phys. Rev. **100**, 181 (1955).
[25] T. Lauritsen and F. Ajzenberg-Selove, Nucl. Phys. **11**, 1 (1959).
[26] L. C. McDermott, K. W. Jones, H. Smotrich, and R. E. Benenson, Phys. Rev. **118**, 175 (1960).
[27] J. D. Pearson, E. Almqvist, and J. A. Kuehner, Can. J. Phys. **42**, 489 (1964).
[28] W. E. Hunt, M. K. Mehta, and R. H. Davis, Phys. Rev. **160**, 782 (1967); M. K. Mehta, W. E. Hunt, and R. H. Davis, *ibid.* **160**, 791 (1967).

TABLE V. Residues of $\bar{S}(\lambda,k)$ at $\lambda=\lambda_n$ corresponding to the pole representation indicated for $He^4(\alpha,\alpha)He^4$ at different incident energies. $B_n=2ik\beta_n$.

E_α(lab) (MeV)	ReB_n	ImB_n	Rep.
3.0	7.128×10^{-3}	0.229	RC
6.0	4.05×10^{-2}	0.495	RC
6.96	0.449	0.366	NK
7.88	0.507	0.389	NK
12.3	0.780	0.383	NK
17.8	0.986	0.413	NK
22.9	1.144	0.451	NK

those corresponding to Table III give a better fit to the experimental cross sections in the incident energy range 10–14 MeV. The trajectories obtained from Table IV are shown in Fig. 4. Both these sets of trajectories failed to give a good fit to the experimental cross sections at higher energies.

IV. RESULTS AND DISCUSSION

In this section we discuss the results of the calculations of differential cross sections given by

$$d\sigma/d\Omega=|A(k,\cos\theta)|^2,$$

using the Regge-pole parameters through various Regge-type representations for $a(\lambda,k)$. The results obtained by this method are compared with experimental data and also with the results obtained by using the smooth cutoff model or Ackhiezer-Pomeranchuk-Blair-McIntyre (APBM)[17,28] model in the case of α-C^{12} and α-O^{16} scattering.

RC denotes the Regge representation modified for Coulomb threshold behavior for which $F(\lambda',\lambda)$ is given by Eq. (2.13). Since we expect that the potential between the projectile and target in nuclear scattering has a Saxon-Woods radial dependence except for very low energies, we use the representations NK having the form given by Eq. (2.22), and N_m given by Eq. (2.23). The results for $m=0$ have quantitative agreement with those of NK. The further modified Regge representation given by Eq. (2.24), with $F(\lambda',\lambda)$ of the form of Eq. (2.23), has the correct asymptotic and threshold behavior and gives the correct zeros. The smallness of the background integral is taken care of by the damping factor $[2\lambda/(\lambda+\lambda')]^m$. The factor N in this representation is taken to be equal to the number of Regge poles considered in computing the scattering amplitudes. The results for this representation are almost quantitatively similar to those of N_m at the energies that are studied. In the case of NK and the modified Regge representations, the factor ξ is calculated from Eq. (2.6) using $\mu_0=a^{-1}$, the value of R is given by Eq. (2.17), and the diffuseness parameter a_0 is taken to be equal to 0.55 F.

The residues at different incident energies for the α-C^{12} and α-O^{16} systems are given in Tables V–VII, respectively. These values correspond to the representation that has yielded the best angular distribution at that energy. Figure 5 shows the angular distributions for $He^4(\alpha,\alpha)He^4$ at different incident laboratory energies, calculated from experimental phase shifts,[29,30] along with the best results obtained from the pole representation. These curves show that at $E_\alpha=3.0$ MeV [see Fig.

TABLE VI. Residues of $\bar{S}(\lambda,k)$ at $\lambda=\lambda_n$ corresponding to the pole representation indicated for $C^{12}(\alpha,\alpha)C^{12}$ at different incident energies. $B_n=2ik\beta_n$.

E_α(lab) (MeV)	Trajectory	ReB_n	ImB_n	Rep.
4.0	I	2.0×10^{-5}	0.005	N_2
	II	6.4×10^{-6}	0.007	
4.745	I	1.2×10^{-6}	0.012	N_2
	II	2.2×10^{-5}	0.013	
11.74	I	-7.0×10^{-2}	0.098	N_2
	II	7.28×10^{-3}	0.118	
	III	5.37×10^{-2}	0.083	
	IV	4.5×10^{-4}	0.011	
	V	-5.0×10^{-4}	0.007	
12.1	I	-5.94×10^{-2}	0.098	N_2
	II	7.7×10^{-3}	0.124	
	III	4.07×10^{-2}	0.097	
	IV	6.5×10^{-4}	0.014	
	V	7.1×10^{-4}	0.008	
14.0	I	-3.65×10^{-2}	0.104	N_2
	II	8.13×10^{-3}	0.155	
	III	5.39×10^{-3}	0.189	
	IV	3.67×10^{-3}	0.030	
	V	-5.06×10^{-3}	0·210	
18.0	II	-1.87×10^{-2}	0.199	N_2
	III	-2.69×10^{-2}	0.600	
	IV	5.49×10^{-2}	0.055	
	V	-4.2×10^{-2}	0.110	
18.5	II	-3.27×10^{-2}	0.200	N_2
	III	2.28×10^{-2}	0.689	
	IV	6.7×10^{-2}	0.050	
	V	-5.73×10^{-2}	0.127	

TABLE VII. Residues of $\bar{S}(\lambda,k)$ at $\lambda=\lambda_n$ corresponding to the pole representation indicated for $O^{16}(\alpha,\alpha)O^{16}$ at different incident energies. $B_n=2ik\beta_n$.

E(lab) (MeV)	Trajectory	ReB_n	ImB_n	Rep.
6.97	I	-7.9×10^{-3}	0.084	NK
	II	-2.7×10^{-3}	0.014	
	III	1.9×10^{-4}	0.0054	
	IV	-7.5×10^{-4}	0.028	
9.92	I	1.85×10^{-3}	0.041	N_2
	II	$-1·8\times10^{-3}$	0.027	
	III	3.2×10^{-3}	0.012	
	IV	3.99×10^{-3}	0.091	
10.05	I	1.88×10^{-3}	0.018	N_2
	II	1.96×10^{-3}	0.064	
	III	4.9×10^{-3}	0.015	
	IV	6.4×10^{-3}	0.11	
11.97	I	0.117	0.046	N_2
	II	0.049	0.008	
	III	0.033	0.007	
	IV	0.393	0.502	
13.37	I	−0.016	0.164	RC
	II	0.015	0.062	
	III	0.003	0.038	

[29] T. A. Tombrello and L. S. Senhouse, Phys. Rev. **129**, 2252 (1963), and references therein.

[30] R. Nilson, W. K. Jentschke, G. R. Briggs, R. O. Kerman, and J. N. Snyder, Phys. Rev. **109**, 850 (1958).

5(a)], a satisfactory fit with experiment is obtained for forward (and hence backward) angles, but not for the intermediate range. At $E_\alpha=6.0$ and 6.96 MeV [see Figs. 5(b) and 5(c)] the fit is satisfactory for the entire range of angles. This clearly shows that at energies in the neighborhood of the 2^+ resonance, the agreement with experiment is quite good. At $E_\alpha=7.88$ MeV [Fig. 5(d)] there is only fair agreement between the experimental and theoretical curves, which gradually becomes worse for higher energies [Figs. 5(e)–5(g)]. This corrob-

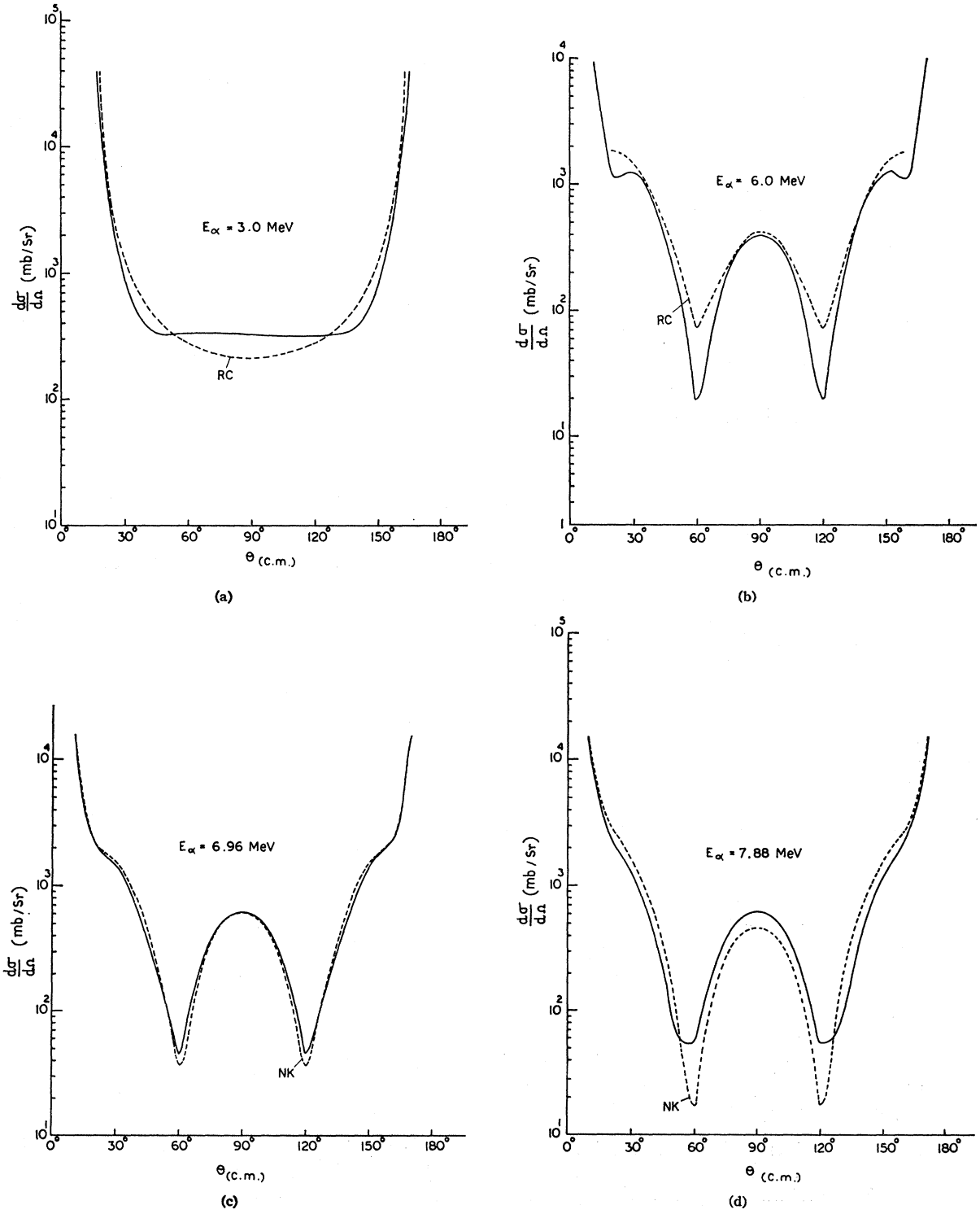

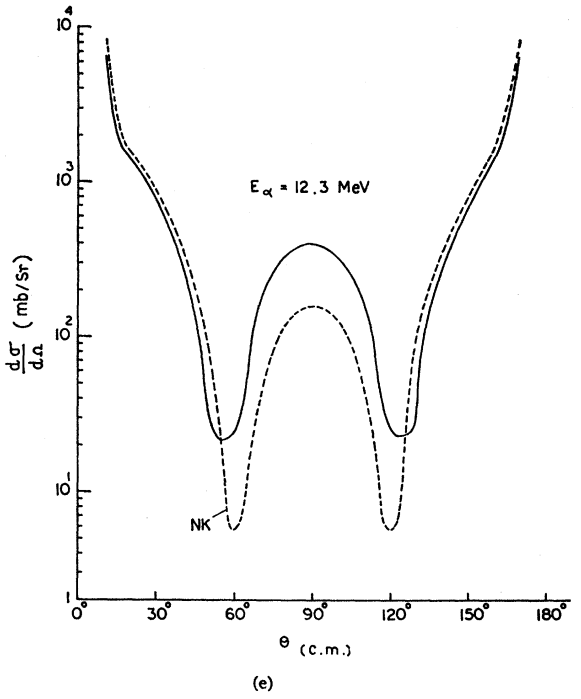

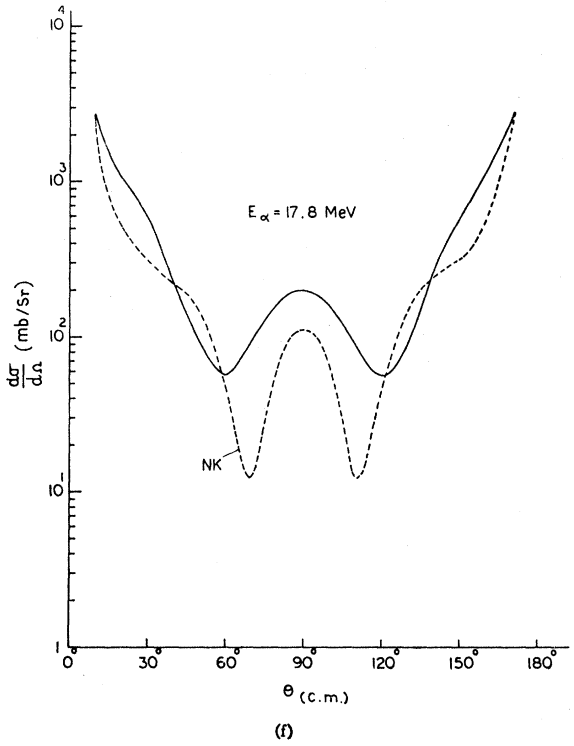

orates Treacy's[15] observation that above $E_\alpha=8$ MeV the one trajectory approximation probably breaks down.

Figures 6(a) and 6(b) illustrate the angular distributions at $E_\alpha=4.0$ and 4.745 MeV, respectively, for C^{12}-$(\alpha,\alpha)C^{12}$ calculated from experimental phase shifts[31] along with that obtained from pole representation. There is fair agreement with experiment up to $\theta_{c.m.}=130°$, but becomes worse for backward angles. Figures 6(c)–6(g) show the angular distributions for $C^{12}(\alpha,\alpha)C^{12}$ corresponding to experiment, the APBM model with resonant phase shifts,[17] and pole representations. The prominant resonances at $E_\alpha=12.1$, 18.0, and 18.5 MeV (see Table II) produce many maxima and minima in the experimental angular-distribution plots. Earlier workers[32–34] observed that at energies 18–19 MeV the differential cross section increases sharply from 165 to to 179°. The angular distributions calculated from pole representations reproduce all these features [see Figs. 6(d), 6(f), and 6(g)]. At $E_\alpha=18.0$ MeV [Fig. 6(f)], the maxima of the differential cross sections were found to occur at nearly constant intervals at angles of about 35, 57, 79, 101, 124, and 149°. The pole-representation curves reproduce all these maxima except the ones at 57 and 79°. Instead, we get a maximum at about 62°. Away from resonances, for instance, at $E_\alpha=11.74$ and

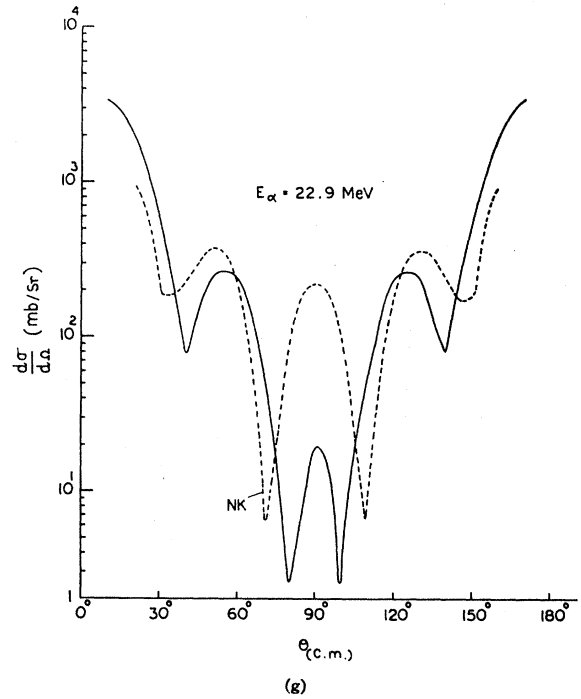

FIG. 5. $He^4(\alpha,\alpha)He^4$ angular distributions at different incident energies. Solid lines correspond to angular distribution from experimental phase shifts, and the dashed line indicates the same from λ-plane pole representation. The symbols designating the various representations are described in Sec. IV.

[31] G. J. Clark, D. J. Sullivan, and P. B. Treacy, Nucl. Phys. **A110**, 481 (1968).
[32] S. Wong and E. Bleuler, Phys. Rev. **125**, 280 (1962).
[33] J. S. Corelli, E. Bleuler, and D. J. Tendem, Phys. Rev. **116**, 1184 (1959).
[34] J. C. Jodogne, P. C. Macq, and J. Steyaert, Phys. Letters **2**, 325 (1962).

14.0 MeV [see Figs. 6(c) and 6(e)], the agreement with experiment improves for backward angles. At all these energies considered it is seen that the representation N_2 with exact ξ yields the best results.

Figure 7 illustrates the angular distributions for $O^{16}(\alpha,\alpha)O^{16}$ corresponding to experiment, the APBM model with resonant phase shifts, and pole representations. The first set of Regge trajectories (see Table III) has been used to calculate the angular distributions at the energies $E_\alpha=9.92$, 11.97, and 13.37 MeV. At $E_\alpha=9.92$ MeV the method N_2 yields tolerable results. At 11.97 MeV, the angular distribution calculated from the pole representations reproduces all the maxima and minima, but the peaks of the maxima are a little displaced. At 13.37 MeV the representation RC yields fair agreement with experiment. The second set of trajectories (see Table IV) has been used to calculate the angular distributions at 6.97 and 10.05 MeV. At 6.97 MeV the pole representations NK and N_0 produce fair agreement with experiment for forward angles, and the agreement greatly improves for backward angles. The angular distributions at $E_\alpha=10.05$ MeV calculated from N_2 also shows a satisfactory fit with experiment for backward angles.

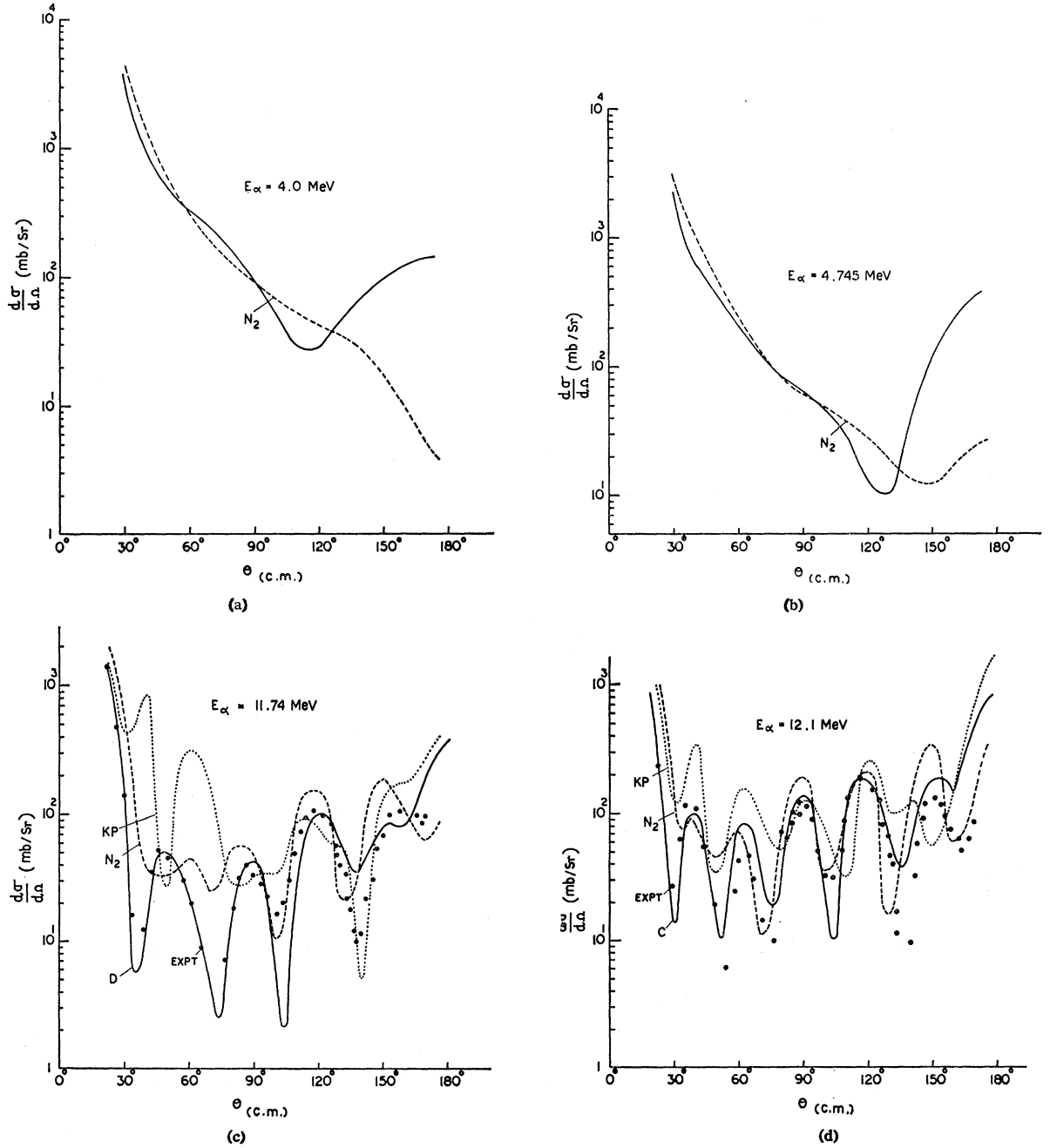

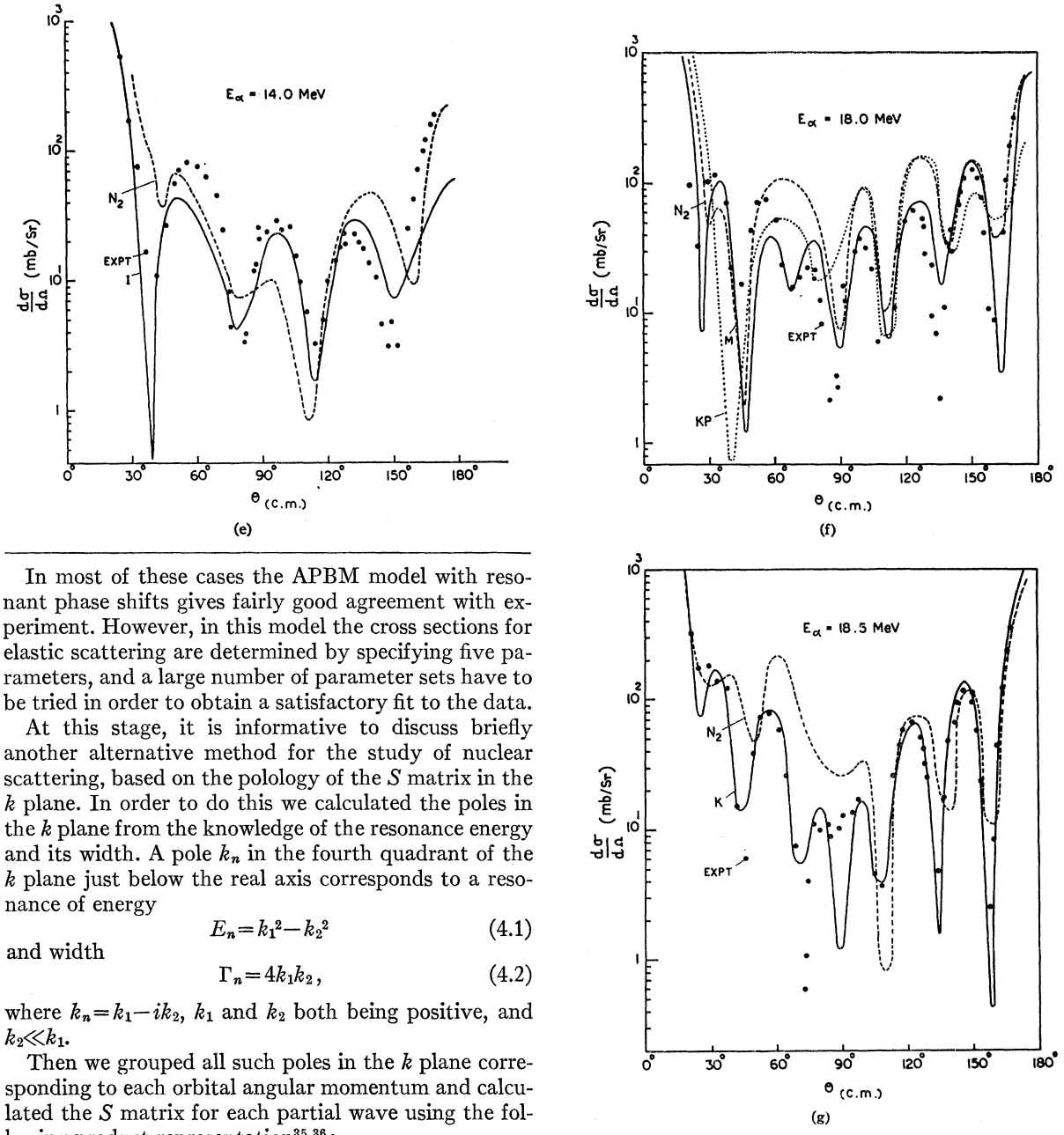

FIG. 6. $C^{12}(\alpha,\alpha)C^{12}$ angular distributions at different incident energies. Conventions similar to those of Fig. 5 are followed. In Figs. 6(c)–6(g) solid circles denote experimental results, the solid line corresponds to the results from the APBM model with resonant phase shifts as given in Ref. 17, the dashed line indicates the angular distribution from λ-plane pole representation, and the dotted line indicates the same from k-plane pole representation given by Eq. (4.3).

In most of these cases the APBM model with resonant phase shifts gives fairly good agreement with experiment. However, in this model the cross sections for elastic scattering are determined by specifying five parameters, and a large number of parameter sets have to be tried in order to obtain a satisfactory fit to the data.

At this stage, it is informative to discuss briefly another alternative method for the study of nuclear scattering, based on the polology of the S matrix in the k plane. In order to do this we calculated the poles in the k plane from the knowledge of the resonance energy and its width. A pole k_n in the fourth quadrant of the k plane just below the real axis corresponds to a resonance of energy

$$E_n=k_1^2-k_2^2 \tag{4.1}$$

and width

$$\Gamma_n=4k_1k_2, \tag{4.2}$$

where $k_n=k_1-ik_2$, k_1 and k_2 both being positive, and $k_2\ll k_1$.

Then we grouped all such poles in the k plane corresponding to each orbital angular momentum and calculated the S matrix for each partial wave using the following product representation[35,36]:

$$\tilde{S}_l(k)=e^{-2ikR}\prod_B\left(\frac{k-k_B^*}{k-k_B}\right)\prod_n\frac{(k+k_n)(k-k_n^*)}{(k-k_n)(k+k_n^*)}, \tag{4.3}$$

where R denotes the radius of the scatterer, B the bound-state poles, and n the resonances. We used this product representation (KP) in preference to the alternative one involving sum over poles, because this does not need the evaluation of residues. In this calculation for $C^{12}(\alpha,\alpha)C^{12}$, all the poles in the E plane[17,22,23] are used. The results of angular distribution obtained by using this procedure (KP) are shown in Figs. 6(c), 6(d), and 6(f) for the case of $C^{12}(\alpha,\alpha)C^{12}$ at $E_\alpha=11.74$, 12.1, and 18.0 MeV.

From these results it is clear that the λ-plane results are, in general, better than those of the k-plane approach, even though exceptions at some energies (see Fig. 8) cannot be ruled out. It should be noted, however,

[35] R. G. Newton, J. Math. Phys. 1, 319 (1960).
[36] H. M. Nussenzveig, in *Analytic Properties of Non-Relativistic Scattering Amplitudes*, edited by J. M. Lozano and L. Sartori (University of Mexico, 1962), p. 57.

that in the k plane we have to consider a larger number of poles than in the λ plane. For example, in the analysis of $C^{12}(\alpha,\alpha)C^{12}$ in terms of poles in the k plane, we used three poles of $l=0$, six of $l=1$, six of $l=2$, five of $l=3$, eight of $l=4$, five of $l=5$, two of $l=6$, and one pole of $l=7$, whereas in the λ plane we had to use only a maximum number of five poles corresponding to five trajectories. In other words, a small number of poles in the right-half λ plane can generate the effect of a large number of poles in the k plane as far as the study of cross sections is concerned. These aspects, together with the comparative discussion of λ-plane and k-plane ap-

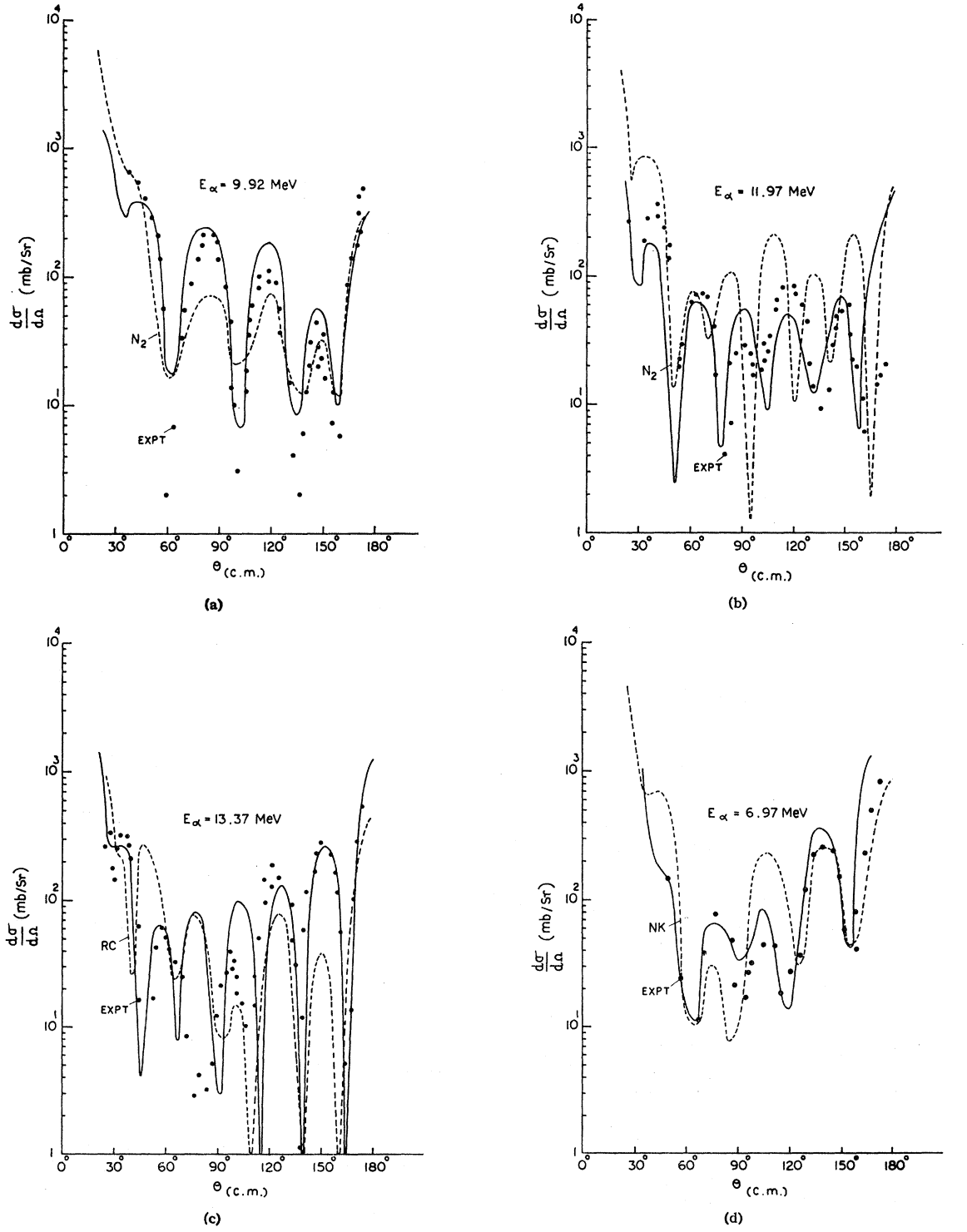

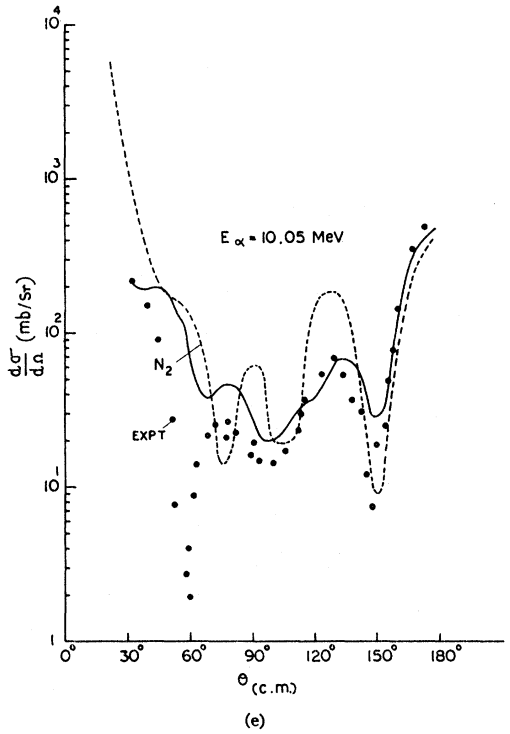

FIG. 7. $O^{16}(\alpha,\alpha)O^{16}$ angular distributions. The conventions of Figs. 5 and 6 are followed. In Figs. 7(a) and 7(d) the solid line corresponds to the results obtained from a phase-shift analysis, and in Figs. 7(b), 7(c), and 7(e) to the results from the APBM model with resonant phase shifts as given in Ref. 28.

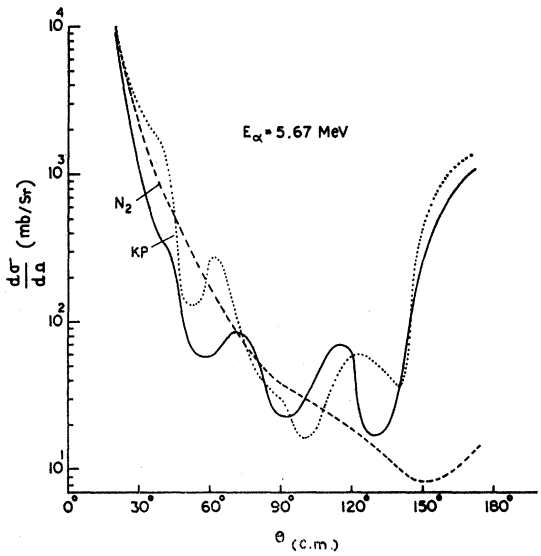

FIG. 8. $C^{12}(\alpha,\alpha)C^{12}$ angular distribution. The conventions of Fig. 6 are followed. Here the solid line indicates the angular distribution from experimental phase shifts (Ref. 31).

proaches to nuclear scattering, establish the usefulness of complex angular-momentum methods.

Before concluding this discussion, we wish to emphasize that the present scheme of calculations is strictly valid when only the elastic channel is open. When one makes calculations at energies where the contribution of inelastic channels are also significant, imposition of elastic unitarity on the S matrix is valid only as an approximation. For example, if one takes into account the inelastic channels by introducing an optical potential of complex strength V_0, the unitarity relation obeyed by the corresponding S matrix $S(\lambda,k,V_0)$ is given by[37]

$$S(\lambda,k,V_0)S^*(\lambda^*,k^*,V_0^*)=1. \tag{4.4}$$

Therefore, if λ_n is a pole of $S(\lambda,k,V_0)$, then λ_n^* is not necessarily a zero. Thus when inelastic channels are open the residues cannot be calculated in terms of poles by solving Eq. (2.26), which is obtained by using the property that λ_n^* is a zero of $S(\lambda,k)$. However, the deviation of $|S(\lambda,k,V_0)|$ from unity gives a measure of the inelastic effects; therefore, we can expect that when $1-|S(\lambda,k,V_0)|$ is small compared to unity, the imposition of elastic unitarity may still be a reliable approximation. In the case of α-α scattering, the inelastic threshold is at 17.25 MeV, and in the case of the α-C^{12} system the inelastic effects are small $[|S(\lambda,k,V_0)|\simeq 1]$ in the energy range that we have considered. However, in the case of the α-O^{16} system, it is observed that for $E_\alpha > 10$ MeV the inelastic cross sections become significant and can no longer be neglected; therefore, imposition of elastic unitarity is likely to introduce errors in the residues. The comparatively worse results for α-O^{16} scattering, particularly at higher energies, may be partly attributed to this source of error. It should also be noted that the inelastic effects, if significant, introduce errors only in our values of the residues, and leave the determination of the other pole parameters unaffected.

Summarizing, it is found that systematics of compound nuclear levels of an elastic-scattering system can be used to analyze nuclear scattering through suitable Regge-type representations without introducing arbitrary parameters. One may, perhaps, improve the results further if R and a_0 are treated as parameters. Moreover, a more detailed and reliable set of resonances and widths can be used to explain the differential cross sections through a Regge representation without introducing a phenomenlogical potential model. In addition, it may be possible to predict the quantum number of certain levels, at least empirically, from an extrapolated Regge trajectory.

ACKNOWLEDGMENTS

The authors wish to express their deep gratitude to Professor S. Mukherjee for his constant encouragement and illuminating discussions on Regge-pole theory. They are grateful to Professor M. K. Pal for his continued interest and helpful advice. They also thank Dr. S. C. K. Nair for some useful suggestions. The computing facilities provided by the Tata Institute of Fundamental Research, Bombay, are also gratefully acknowledged.

[37] S. Mukherjee and C. S. Shastry, Nucl. Phys. (to be published).